Biochimica et Biophysica Acta 1840 (2014) 2310–2320

Contents lists available at ScienceDirect

Biochimica et Biophysica Acta

journal homepage: www.elsevier.com/locate/bbagen

Cell death caused by quinazolinone HMJ-38 challenge in oral carcinoma CAL 27 cells: dissections of endoplasmic reticulum stress, mitochondrial dysfunction and tumor xenografts

Chi-Cheng Lu [a], Jai-Sing Yang [b], Jo-Hua Chiang [a], Mann-Jen Hour [c], Kuei-Li Lin [d], Tsung-Han Lee [a,e,*], Jing-Gung Chung [e,f,**]

[a] Department of Life Sciences, National Chung Hsing University, Taichung 40227, Taiwan
[b] Department of Pharmacology, China Medical University, Taichung 40402, Taiwan
[c] School of Pharmacy, China Medical University, Taichung 40402, Taiwan
[d] Department of Radiation Oncology, Chi Mei Medical Center, Tainan 71004, Taiwan
[e] Department of Biological Science and Technology, China Medical University, Taichung 40402, Taiwan
[f] Department of Biotechnology, Asia University, Taichung 41354, Taiwan

ARTICLE INFO

Article history:
Received 19 August 2013
Received in revised form 26 January 2014
Accepted 18 February 2014
Available online 1 March 2014

Keywords:
HMJ-38
Human oral carcinoma cells
Endoplasmic reticulum stress
Mitochondrial dysfunction
Tumor xenografts

ABSTRACT

Background: This investigation clearly clarified the synthesized and antimitotic compound, 2-(3′-methoxyphenyl)-6-pyrrolidinyl-4-quinazolinone (HMJ-38), addressing its target and precise mechanism of action. We hypothesized that HMJ-38 might sensitize apoptotic death of human oral carcinoma CAL 27 cells *in vitro* and inhibit xenograft tumor growth *in vivo*.
Methods: Cell viability was assessed utilizing MTT assay. HMJ-38-treated cells represented DNA fragmentation using agarose gel electrophoresis as further evidenced using TUNEL staining. Flow cytometric analyses, immunoblotting and quantitative RT-PCR were applied for protein and gene expression. Antitumor xenograft study was employed.
Results: HMJ-38 concentration- and time-dependently reduced viability of CAL 27 cells. The effect of intrinsic molecules was signalized during HMJ-38 exposure with disruption of $\Delta\Psi m$, MPT pore opening and the release of various events from mitochondria undergoing cell apoptosis. HMJ-38 also markedly facilitated G_2/M phase arrest. HMJ-38 stimulated the activation of CDK1 activity that modulated phosphorylation on Ser70 of Bcl-2-mediated mitotic arrest and apoptosis. HMJ-38 triggered intracellular Ca^{2+} release and activated related pivotal hallmarks of ER stress. HMJ-38 in nude mice bearing CAL 27 tumor xenografts decreased tumor growth. Furthermore, HMJ-38 enhanced caspase-3 gene expression and protein level in xenotransplanted tumors.
Conclusions: Early roles of mitotic arrest, unfolded protein response and mitochondria-dependent signaling contributed to apoptotic CAL 27 cell demise induced by HMJ-38. In *in vivo* experiments, HMJ-38 also efficaciously suppressed tumor volume in a xenotransplantation model.
General significance: This finding might fully support a critical event for HMJ-38 *via* induction of apoptotic machinery and ER stress against human oral cancer cells.

1. Introduction

Head and neck squamous cell carcinoma (HNSCC), including oral squamous cell carcinoma (OSCC), is ranked as the sixth most prevalent malignancy worldwide [1,2]. In Taiwan, betel quid chewing is a vital prognostic factor related to oral cancer [3,4]. Over 90% of oral cancer cases are classified as OSCC and associated with a poor prognosis [5,6]. In the clinical treatment options, there are multiple-modality therapies with surgical resection, radiation technique and multi-drug chemotherapy for HNSCC patients [7]. However, the long-term survival has no dramatic increase over the past several years [8]. The clinical outcome (side effect) and poor prognostic factor of OSCC occur, and the therapeutic actions in the end-stage are still unsatisfactory [9,10]. Thus, the discovery of potential and novel chemotherapeutic agents to trigger apoptotic death for HNSCC not only is becoming essential but also has received the increasingly important approach.

Apoptosis or programmed cell death type I (an ability to provoke the physiological suicide program) is a central process of antitumor effects

* Correspondence to: T.–H. Lee, Department of Life Sciences, National Chung Hsing University, 250, Kuo-Kuang Road, Taichung 40227, Taiwan. Tel.: +886 422856141; fax: +886 422851797.
** Correspondence to: J.-G. Chung, Department of Biological Science and Technology, China Medical University, 91, Hsueh-Shih Road, Taichung 40402, Taiwan. Tel.: +886 422053366x2161; fax: +886 422053764.
E-mail addresses: thlee@email.nchu.edu.tw (T.-H. Lee), jgchung@mail.cmu.edu.tw (J.-G. Chung).

http://dx.doi.org/10.1016/j.bbagen.2014.02.022
0304-4165/

to eliminate tumor cells [4,11]. Apoptotic signaling refers to responding to a variety of stressful stimuli or drug treatments, and its related bimolecular switches are defined for the modes of extrinsic signaling (death receptor engagement), intrinsic network (mitochondria-dependent pathway) and endoplasmic reticulum (ER) stress (unfolded protein response, UPR) [12–14]. The accumulation of unfolded and/or misfolded proteins undergoing various stress conditions elicits Ca^{2+} overload and failure of protein synthesis or folding, finally leading to disturb ER function. ER stress triggers several essential hallmarks to be a potential target [13–15]. In addition, UPR-regulated cell apoptosis might get involved in intrinsic mitochondrial signaling by proceeding through the caspase-9/-3-dependent pathway [16–18]. Bcl-2 family proteins have been found to implicate mitochondrial depolarization, and subsequently apoptotic factors emanating from mitochondria are released, following initiator and effector caspases can be eventually activated when the cell dies [19,20].

A class of quinazolinone derivatives was designed and synthesized as a novel antineoplastic agent by our colleagues [21,22]. This synthetic compound, HMJ-38, as shown in Fig. 1A exerts excellent efficacy and therapeutic effect on numerous tumor cell lines after the screening tests for cytotoxic function, indicating the most potent to inhibit tubulin polymerization *in vitro* [22]. We previously demonstrated that intrinsic apoptosis triggered by HMJ-38 appeared in human promyelocytic leukemia HL-60 cells [23]. HMJ-38 was also found to exhibit potential angiogenetic effects and induction of human umbilical vein endothelial cell apoptosis [24]. Presently, neither the cytotoxic influence of HMJ-38 nor the molecular interactions underlying its antitumor activity on HNSCC cells *in vitro* and *in vivo* have been well established. The aim of this study was to elucidate the anticancer mechanism of HMJ-38-induced apoptotic machinery and to investigate ER stress and intrinsic associated signal transduction in human OSCC CAL 27 cells as well as against implanted human oral tumor xenografts in nude mice. Our pilot study hypothesized that HMJ-38 might affect CAL 27 cells, and its cytotoxic response could be attributable to apoptotic cell death. The cell culture and animal models were developed to explore the oral anticancer effects. Therefore, we strongly suggest that HMJ-38 has a therapeutic potential to enhance apoptotic death in human OSCC cells *in vitro* and *in vivo*.

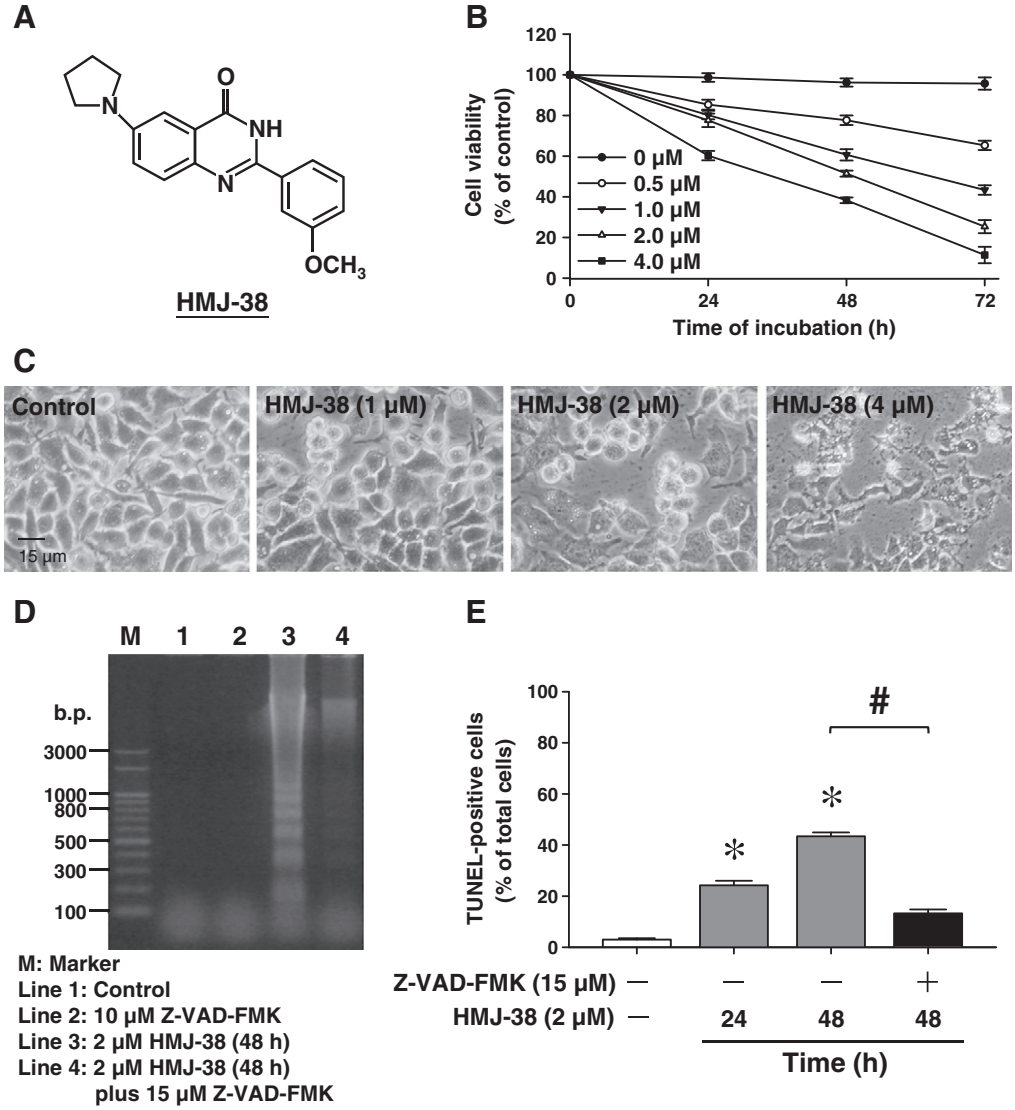

Fig. 1. Correlations of HMJ-38-induced cytotoxic effect and induction of caspase-mediated apoptotic death on CAL 27 cells. (A) Representation of the chemical structure of HMJ-38. Cells prior to preincubation with or without 15 μM Z-VAD-FMK were incubated in the presence of different concentrations of HMJ-38 or exposed to 2 μM HMJ-38 for various lengths of time. (B) Cytotoxic effect on HMJ-38-treated cells was analyzed using MTT method. (C) Cells in response to HMJ-38 for 48 h were photographed. Scale bar = 15 μm. (D) Enrichment of DNA fragmentation was analyzed by agarose gel electrophoresis. (E) TUNEL-positive cells were measured. The data are presented as mean ± S.E.M. (n = 3) and significantly greater than the values obtained by Dunnett's test. *$p < 0.05$ *versus* control; #$p < 0.05$ *versus* HMJ-38 alone.

2. Materials and methods

2.1. Reagents and chemicals

HMJ-38 was supplied by Dr. Mann-Jen Hour (School of Pharmacy, China Medical University). Dulbecco's Modified Eagle Medium (DMEM), DMEM: Nutrient Mixture F-12 (DMEM/F-12), Minimum Essential Medium (MEM), fetal bovine serum (FBS), penicillin/streptomycin and trypsin-EDTA were purchased from Gibco/Life Technologies (Carlsbad, CA, USA). $DiOC_6(3)$, Fluo-3/AM and BAPTA were obtained from Molecular Probes/Life Technologies (Eugene, OR, USA). The source of antibodies as follows: caspase-9, caspase-3, phospho-CDK1 (Thr161), phospho-Bcl-2 (Ser70), eIF2α and phospho-eIF2α (Ser51) as well as calpain 1 were bought from Cell Signaling Technology Inc. (Beverly, MA, USA). Specific caspase inhibitors (Z-VAD-FMK, Z-LEHD-FMK and Z-DEVD-FMK), calpeptin and antibodies of anti-Bax, anti-CDK1 and anti-Bcl-2 were obtained from Merck Millipore (Billerica, MA, USA). The other primary antibodies used in this study and salubrinal were purchased from Santa Cruz Biotechnology, Inc. (Santa Cruz, CA, USA). All chemicals and reagents were obtained from Sigma-Aldrich Corp. (St. Louis, MO, USA) unless otherwise specified.

2.2. Cell lines and culture conditions

Human OSCC cell line CAL 27 was purchased from the American Type Culture Collection (ATCC, Manassas, VA, USA). Human tongue oral cancer cell line SCC-4, human fetal skin fibroblast cell line WS1 and human embryonic skin fibroblast cell line Detroit 551 were purchased from the Bioresource Collection and Research Centre (BCRC) (Hsinchu, Taiwan). CAL 27 cells were cultured with DMEM, SCC-4 cells were grown in DMEM/F-12, and WS1 and Detroit 551 cells were seeded in MEM. All cell lines were plated into T75 tissue culture flasks (TPP Techno Plastic Products AG, Trasadingen, Switzerland) and individually cultured in different media supplemented with 10% (v/v) FBS, 2 mM L-glutamine, 100 Units/ml penicillin and 100 μg/ml streptomycin in a humidified atmosphere containing 5% (v/v) CO_2 and 95% (v/v) air at 37 °C. All cell death assays were performed using the same culture media mentioned above. Cells were detached by 0.25% (w/v) trypsin/0.02% (w/v) EDTA and split every 2–3 days to maintain cell growth [25–27].

2.3. Methyl thiazolyl tetrazolium (MTT) assay

Cell viability was determined utilizing the MTT-based *in vitro* toxicology assay as previously described [28]. In brief, four types of cell lines (CAL 27, SCC-4, WS1 and Detroit 551) were individually plated at a density of 1×10^4 cells/well into 96-well plates and treated with various concentrations (0.5, 1.0, 2.0 and 4.0 μM) of HMJ-38 for 24, 48 and 72 h or dimethyl sulfoxide (DMSO) alone [0.5% (v/v) in media served as a vehicle control]. After treatments, the medium was discarded before a 100-μl solution of MTT (500 μg/ml) was added to each well for 4 h at 37 °C. The supernatant was then replaced by the addition of 200 μl DMSO to solubilize the violet formazan crystal produced from MTT. The absorbance of the dissolved formazan grained within the cells was measured at 570 nm by a microplate reader (Anthos Labtec Instruments GmbH, Salzburg, Austria) to calculate viability (% of control).

2.4. Observation for morphological aspects of apoptosis

CAL 27 cells (2×10^5 cells/well) into 12-well plates were treated in the absence and presence of different concentrations (1, 2 and 4 μM) of HMJ-38. After 48 h, cells were visualized and photographed under a phase-contrast microscope to check apoptotic features before being harvested as described elsewhere [29].

2.5. Terminal deoxynucleotidyl transferase-mediated d-UTP nick end labeling (TUNEL) evaluation by flow cytometry

CAL 27 cells (2×10^5 cells/well) into 12-well plates were individually preincubated in the presence and absence of 20 μM roscovitine (a CDK inhibitor) or 15 μM Z-VAD-FMK (a cell-permeable pan-caspase inhibitor) for 2 h prior to 2 μM HMJ-38 exposure for 24 or 48 h. After incubation, TUNEL assay was employed to detect apoptotic DNA breaks utilizing the *In Situ* Cell Death Detection Kit, Fluorescein (Roche Diagnostics GmbH, Roche Applied Science, Mannheim, Germany), following the protocol provided by the manufacturer. TUNEL-positive cells were analyzed using a BD FACSCalibur Flow Cytometry System (BD Biosciences, San Jose, CA, USA) and BD CellQuest Pro Software.

2.6. DNA fragmentation detection

CAL 27 cells (5×10^6 cells/flask) were pretreated with or without 15 μM Z-VAD-FMK for 2 h and exposed to 2 μM HMJ-38 for 48 h. Cells were thereafter harvested, washed and lysed in 500 μl lysis buffer [20 mM Tris (pH 8.0), 10 mM EDTA and 0.2% (v/v) Triton X-100] at 4 °C for 20 min. These lysed cells were digested overnight with 100 μg/ml proteinase K (AMRESCO Inc., Solon, OH, USA) at 50 °C, following by incubation with 50 μg/ml RNase A at 37 °C for 1 h. DNA fragments were extracted with phenol/chloroform/isopropanol (24:25:1; v/v/v) and precipitated with 50% (v/v) isopropanol with 20 μg/ml glycogen before being re-suspended in 100 μl Tris-EDTA (TE) buffer (AMRESCO Inc.) as the previous reported methods [11,30]. Samples were electrophoresed on 1.8% (w/v) agarose gel in 0.5× Tris-Borate-EDTA (TBE) buffer (AMRESCO Inc.), and DNA was stained with 1 μg/ml ethidium bromide (EtBr). The gel was photographed under a UV lamp.

2.7. Measurements of mitochondrial transmembrane potential ($\Delta\Psi m$) and mitochondrial permeability transition (MPT) pore with calcein by flow cytometry

CAL 27 cells (2×10^5 cells/ml) into 12-well plates were exposed to 2 μM HMJ-38 for 0, 6, 12 and 24 h. At the end of treatments, cells were collected and incubated with 500 μl $DiOC_6(3)$ (a cell-permeant, lipophilic and green-fluorescent dye, 50 nM) at 37 °C for 30 min as described elsewhere [31,32]. To evaluate the opening of MPT pore, the commercially available MitoProbe Transition Pore Assay Kit (Molecular Probes) was applied according to the procedures recommended by the manufacturer. Mean fluorescence intensity (MFI) of confined calcein was monitored after cytosolic fluorescence was quenched by cobalt(II) chloride ($CoCl_2$), and the data are shown as 100% of control for calcein MFI.

2.8. Immunoblot assay

The enhanced chemiluminescence (ECL) immunoblotting was performed to identify the protein levels. Briefly, CAL 27 cells (5×10^6 cells per flask) were treated with 2 μM HMJ-38 for indicated intervals of time (see figure legends), harvested and then lysed in the PRO-PREP Protein Extraction Solution (iNtRON Biotechnology, Seongnam-si, Gyeonggi-do, Korea). Equal loading was verified by determining protein concentration as previously described [29,30], and the samples of cell lysates (40 μg protein) were separated by 10–12% (w/v) sodium dodecyl sulfate (SDS)-PAGE. After being electrophoresed, proteins from the gels were transferred to the Immobilon-P Transfer Membrane (Merck Millipore). The membrane was then hybridized with specific primary antibody at 4 °C overnight after being blocked with PBS containing 0.1% (v/v) Tween 20 and 5% (w/v) nonfat dry milk for 1 h at room temperature. The blots were developed using appropriate horseradish peroxidase (HRP)-conjugated secondary antibodies against rabbit or mouse immunoglobulin (Santa Cruz Biotechnology, Inc.) and visualized utilizing Immobilon Western Chemiluminescent

HRP Substrate (Merck Millipore) and Amersham Hyperfilm ECL (GE Healthcare, Piscataway, NJ, USA). All bands in the blots were normalized to the level of GAPDH or β-actin for each lane. The density of the immunoreactive band was quantified by ImageJ 1.47 program for Windows from the National Institute of Health (NIH) (Bethesda, MD, USA).

2.9. Immunofluorescence staining for cytochrome c trafficking by confocal microscopy

CAL 27 cells (5×10^4 cells/well) were plated into 4-well chamber slides and incubated with vehicle alone (control) and 2 μM HMJ-38 for 24 h. Cells were rinsed, fixed and permeabilized described by Chiang et al. [30]. Subsequently, cells were incubated with anti-cytochrome *c* antibody diluted to 1:100 at 4 °C overnight after being blocked with 2.5% bovine serum albumin (BSA) for 1 h at room temperature, followed labeling with a fluorescein isothiocyanate (FITC)-conjugated anti-mouse-IgG secondary antibody (green fluorescence, Molecular Probes) at 1:200 dilution for 1 h. Afterwards, cells were counterstained with CellTracker Red CMTPX (Molecular Probes) for cytosol. The slides were mounted with coverslips to be visualized, and photomicrographs were then analyzed using a Leica TCS SP2 Confocal Spectral Microscope (Leica Microsystems, Heidelberg, Mannheim, Germany).

2.10. Assessments for caspase-3 and -9 activities

Approximately 5×10^6 CAL 27 cells in T75 flasks were exposed to 2 μM HMJ-38 for 0, 24 and 48 h after pretreatment with or without 15 μM of the selective inhibitors (Z-DEVE-FMK for caspase-3 and Z-LEHD-FMK for caspase-9) for 2 h. Cell lysates were collected and then determined in accordance with the manufacturer's procedures provided in the Caspase-3 and Caspase-9 Colorimetric Assay Kits (R&D System Inc., Minneapolis, MN, USA).

2.11. RNA isolation and quantitative RT-PCR method

CAL 27 cells at a density of 5×10^6 in T75 flasks were incubated with or without 2 μM HMJ-38 for 12 and 24 h. Cells were washed and trypsinized before cell pellets were collected by centrifugation, and total RNA from each treatment was extracted by QIAGEN RNeasy Mini Kit (QIAGEN Inc., Valencia, CA, USA). RNA purity was assessed as previously described [30], and RNA samples were then individually reverse-transcribed using the High Capacity cDNA Reverse Transcription Kits (Applied Biosystems, Foster City, CA, USA). Quantitative PCR from each sample was exploited for amplifications with 2× SYBR Green PCR Master Mix (Applied Biosystems) and 200 nM of forward and reverse primers for each gene as listed in Table S1 as previously reported [30,33,34]. Each assay was measured in triplicate using an Applied Biosystems 7300 Real-Time PCR System, and the value was expressed in the comparative threshold cycles (C_T) method for the housekeeping gene GAPDH.

2.12. DNA content by flow cytometric analysis

CAL 27 cells at a density of 2×10^5 cells/well were subcultured into 12-well plates and treated with 2 μM HMJ-38 for 0, 12, 24 and 48 h. After challenge, cells were harvested by trypsinization, washed twice with PBS and fixed in 70% (v/v) ethanol at −20 °C overnight. Afterwards, cells were incubated in the presence of 500 μl PBS with 0.1% (v/v) Triton X-100, 100 μg/ml RNase A and 40 μg/ml PI for 30 min in constant darkness as previously described [29,33]. Cell cycle distribution and sub-G_1 population containing apoptotic cells were subjected to flow cytometric analysis.

2.13. Cyclin-dependent kinase 1 (CDK1) activity assay

CAL 27 cells at a density of 5×10^6 per T75 flask were incubated with 2 μM HMJ-38 for 0, 3, 6, 12 and 24 h. Cells were harvested, and the ability of CDK1 kinase activity from cell extracts prepared from each treatment was thereby measured according to the instructions of the manufacturer (CycLex Cdc2-Cyclin B Kinase Assay Kit, MBL International Corp., Woburn, MA, USA).

2.14. Determination of intracellular Ca^{2+} level

Approximately 2×10^5 CAL 27 cells per well into 12-well plates were exposed to 2 μM HMJ-38 for various time periods (0, 6, 12 and 24 h) before being harvested, washed twice and re-suspended in 500 μl Fluo-3/AM (a Ca^{2+} indicator, 2.5 μg/ml) at 37 °C for a 40-min incubation as described elsewhere [7,30]. The loaded cells were then immediately detected the influence of fluorescence intensity on intracellular Ca^{2+} release and analyzed by flow cytometry.

2.15. Assay for calpain activity

CAL 27 cells (5×10^6 cells/flask) plated into T75 flasks were treated with 2 μM HMJ-38 for 0, 12, 24 and 48 h, and calpain activity was assayed using a fluorogenic calpain substrate (Suc-Leu-Leu-Val-Tyr-AMC, proteasome substrate) (Enzo Life Sciences, Farmingdale, NY, USA) as previously described [35–37]. After that, proteolytic hydrolysis of cellular fluorescence was monitored and quantified by the Perkin-Elmer HTS 7000 Series BioAssay Reader (Boston, MA, USA) with filter settings with 360-nm excitation and 460-nm emission.

2.16. Implications of inhibitors for CDK1 and ER stress-related signaling on cell viability and alterations of protein levels triggered by HMJ-38

CAL 27 cells were exposed to 2 μM HMJ-38 for indicated time after preincubation in the presence and absence of 20 μM roscovitine, 5 μM BAPTA (a Ca^{2+} chelator), 10 μM calpeptin (a cell permeable calpain inhibitor) or 10 μM salubrinal (an eIF2α dephosphorylation inhibitor) for 2 h, respectively, followed by determination for viability utilizing MTT assay as detailed above. For measuring relative protein levels, cells were individually pretreated with 20 μM roscovitine or 10 μM calpeptin for 2 h and thereafter incubated with 2 μM HMJ-38 for 24 h. After treatment, cells were harvested to detect protein levels utilizing immunoblot assay as stated above.

2.17. Animals' experimentation

All animal experiments complied with institutional guidelines (Affidavit of Approval of Animal Use Protocol, No. 100-212-C) approved by the Institutional Animal Care and Use Committee (IACUC) of China Medical University (Taichung, Taiwan). All pathogen-free five-week-old male BALB/c athymic nude mice were purchased from the National Laboratory Animal Center (Taipei, Taiwan). The animals were housed at a constant room temperature with a regular 12-h light/12-h dark cycle and hereafter fed a standard rodent diet and water *ad libitum*.

2.18. Xenograft antitumor study

CAL 27 cells (1×10^7 cells/mouse) in 0.2 ml at 1:1 mixture of cultural medium and BD Matrigel Basement Membrane Matrix (BD Biosciences, Bedford, MA, USA) were subcutaneously injected into the flank of nude mice to form a solid tumor as described elsewhere [4,7,25]. When xenograft tumors reached approximately 200 mm^3 (at day 22 after cell inoculation), twenty-four mice were randomly divided into three groups with eight ones in each group. The experimental treatments by intraperitoneal (i.p.) injection included HMJ-38 at the dosages of 1 and 2.5 mg/kg body weight, respectively, every other day ten times

Table 1
Summary of HMJ-38 for *in vitro* cytotoxicity of human oral cancer and non-cancer fibroblast cell lines.[a]

Cell lines	IC_{50} (μM)
CAL 27 (human oral squamous cell carcinoma cells)	2.50 ± 0.60
SCC-4 (human tongue cancer cells)	4.68 ± 0.28
WS1 (human fetal skin fibroblast cells)	>100
Detroit 551 (human embryonic skin fibroblast cells)	>100

[a] Cells were exposed to various concentrations of HMJ-38 for 48 h. After incubation, cells were determined for viability by MTT assay as described in Materials and methods. The IC_{50} value of HMJ-38 at a 48-h exposure was shown from a concentration–response curve of each cell line and expressed as mean ± S.E.M. of triplicate determinations from at least three independent experiments.

(dosing regimen: Q2D × 10, i.p.), whereas control mice were intraperitoneally received with 30 μl DMSO throughout the experimental period. The tumor size (mm^3) from each mouse was calculated utilizing a caliper by the following formula: 0.5 × length × $(width)^2$. At the end of treatment, all animals were anesthetized by carbon dioxide (CO_2) and sacrificed on the 40th day. The tumor tissues from each mouse were measured and individually weighed after being removed. The tumors were processed according to the previous stated methods [33,38] and evaluated by quantitative RT-PCR and immunoblotting as mentioned earlier.

2.19. Statistical analysis

The results are expressed as mean ± standard error of the mean (S.E.M.) in triplicate. Each analysis was exploited on the data using one-way analysis of variance (ANOVA) followed by Dunnett's test between the treated and untreated group(s). The level of statistical significance was considered as a probability (p) value < 0.05.

3. Results

3.1. HMJ-38 is cytotoxic to human oral carcinoma cells and provokes the caspase-mediated apoptotic characteristic in CAL 27 cells

The cytotoxic potential represented different types of cell lines (oral cancer and non-cancer cells) cultured in the presence of HMJ-38 as summarized in Table 1. HMJ-38 exhibited an excellent and more toxic effect on CAL 27 cells than that on SCC-4 cells (CAL 27 > SCC-4). HMJ-38 had less sensitive (IC_{50} > 100 μM) to the non-cancer cell lines (human fetal skin fibroblast WS1 cells and embryonic skin fibroblast

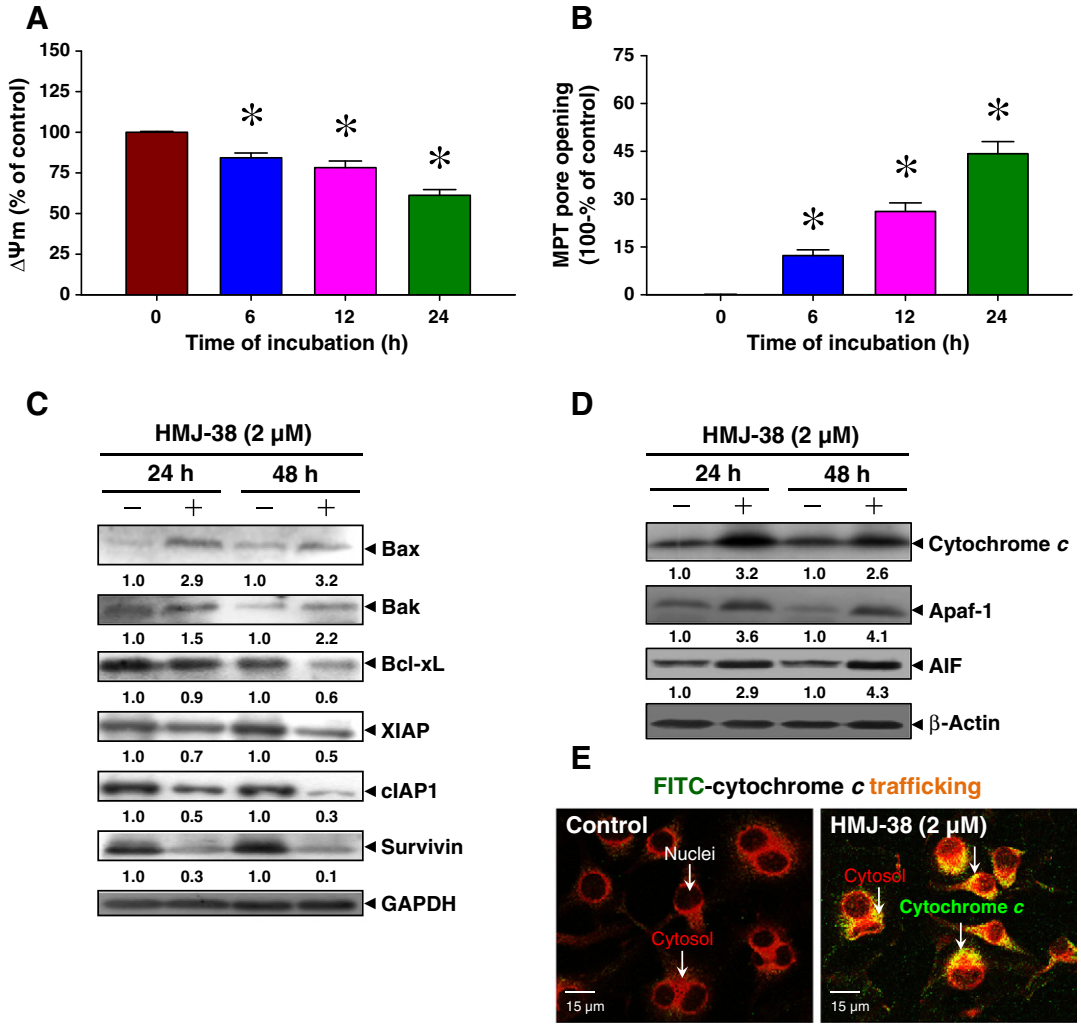

Fig. 2. HMJ-38 provokes mitochondrial dysfunction and influences Bcl-2 family proteins during CAL 27 cell apoptosis. Cells were treated with 2 μM HMJ-38 for indicated lengths of time. (A) The disruption of ΔΨm was measured by using the fluorochrome $DiOC_6(3)$ and flow cytometry. (B) MPT pore opening was determined utilizing MitoProbe Transition Pore Assay Kit. Results are plotted as mean ± S.E.M. (n = 3) and found significantly different by Dunnett's test. *p < 0.05 *versus* untreated control. Cell lysates were subjected to immunoblot analysis. (C) Cell fractions were probed with anti-Bax, -Bak, -Bcl-xL, -XIAP, -cIAP1 and -survivin antibodies. (D) The expressions of cytochrome *c*, Apaf-1 and AIF protein levels were detected as described in Materials and methods. (E) Trafficking cytochrome *c* was visualized after a 24-h exposure. The overlapped micrographs (yellow) were merged from immunofluorescence staining of cytochrome *c* (green, FITC-labeled) and cytosol (red, CellTracker Red CMTPX-stained). Scale bar = 15 μm.

Detroit 551 cells). Trypan blue exclusion assay was exploited to confirm the viability in these multiple cell lines. Consistent with our earlier study, HMJ-38 exerts less cytotoxicity in normal human peripheral blood mononuclear cells (PBMC) [23]. Hence, the cytotoxic effect of HMJ-38 was further investigated. HMJ-38 decreased the percentage of viable CAL 27 cells in a concentration- and time-dependent manner (Fig. 1B), and the half maximal inhibitory concentration (IC_{50}) value after a 48-h treatment was 2.50 ± 0.60 μM. Hence, we chose HMJ-38 at the concentration of 2 μM for further examinations in this study.

We further questioned whether the cytotoxic response of HMJ-38 causes apoptotic death on CAL 27 cells. Cells after HMJ-38 treatment were subjected to concentration-dependent morphological changes, like cell shrinkage, rounding and membrane blebbing as well as substantial apoptotic cell death (Fig. 1C). DNA ladder pattern (a typical pattern of internucleosomal fragmentation for apoptosis) was visualized in HMJ-38-treated cells (Fig. 1D). In support of the apoptotic response *in vitro*, we next examined DNA breaks *in vitro*. HMJ-38 exposure for 24 and 48 h stimulated the appearance of TUNEL-positive cells in a time-course pattern (Fig. 1E). We also used Z-VAD-FMK to test the caspase dependence of HMJ-38-induced killing of CAL 27 cells. Preincubation with Z-VAD-FMK could protect against HMJ-38-fragmented DNA (Fig. 1D) and reduce the number of TUNEL-positive population (Fig. 1E). Based on our findings, HMJ-38-induced cell death was mediated by way of the caspase-dependent apoptotic pathway in CAL 27 cells *in vitro*.

3.2. HMJ-38-induced apoptosis of CAL 27 cells is mediated through the mitochondrial death effectors and caspase cascade-dependent mechanism

To address how cellular signals of mitochondrial modulation interact with HMJ-38-induced apoptosis, we determined experimentally the levels of apoptosis-related protein and mRNA expressions. Mitochondria possess the death effectors when controlling cell apoptosis. The various pivotal elements (cytochrome *c*, Apaf-1, pro-caspase-9 and AIF) are released from mitochondria during a loss of inner mitochondrial membrane permeability [12,39]. HMJ-38 time-dependently collapsed ΔΨm (Fig. 2A) and enhanced opening of MPT pore (Fig. 2B) within 24 h. The depolarized ΔΨm and mitochondrial dysfunction are conducted through regulating Bcl-2 family signals and conveying caspases in proteolytic cascade [40–42]. To verify further downstream of dissipation for ΔΨm, we first examined the effects of HMJ-38 on Bcl-2 family molecules, mitochondria-released proteins and intrinsic caspase proteases. The protein levels of Bcl-xL, X-linked inhibitor of apoptosis (XIAP), cellular inhibitor of apoptosis proteins 1 (cIAP1) and survivin were decreased, while those of Bax and Bak were increased in HMJ-38-treated cells in a time-dependent manner (Fig. 2C). The release of cytochrome *c*, Apaf-1 and AIF protein levels from mitochondria were enhanced after HMJ-38 treatment (Fig. 2D). The trafficking cytochrome *c* was translocated from mitochondria to cytosol in HMJ-38-challenged CAL 27 cells (Fig. 2E).

To check whether HMJ-38-provoked apoptosis is carried out *via* the intrinsic pathway, cells were preincubated with or without individual specific inhibitors of caspase-3 (Z-DEVD-FMK) and caspase-9 (Z-IETD-FMK) before incubation with HMJ-38. HMJ-38 at 24 and 48-h exposures stimulated caspase-3 and caspase-9 activities in a time-effect plot, and both caspase protease inhibitors substantially neutralized proapoptotic activity when compared to the HMJ-38-treated only sample (Fig. 3A and B). Each protein level of caspase-9 and caspase-3 were cleaved into active form in HMJ-38-treated cells (Fig. 3C). Alternatively, the levels of *caspase-3*, *caspase-9* and *AIF* gene expression were prompted after HMJ-38 treatment (Fig. 3D). Altogether, these results seem to demonstrate that manifestation of CAL 27 cell apoptosis occurred by way of the mitochondrial signaling and activation of intrinsic caspases by HMJ-38. Herein, we summarize the current understanding of the function in HMJ-38-treated CAL 27 cells that elicited apoptosis *via* the mitochondria-dependent caspase cascade signals.

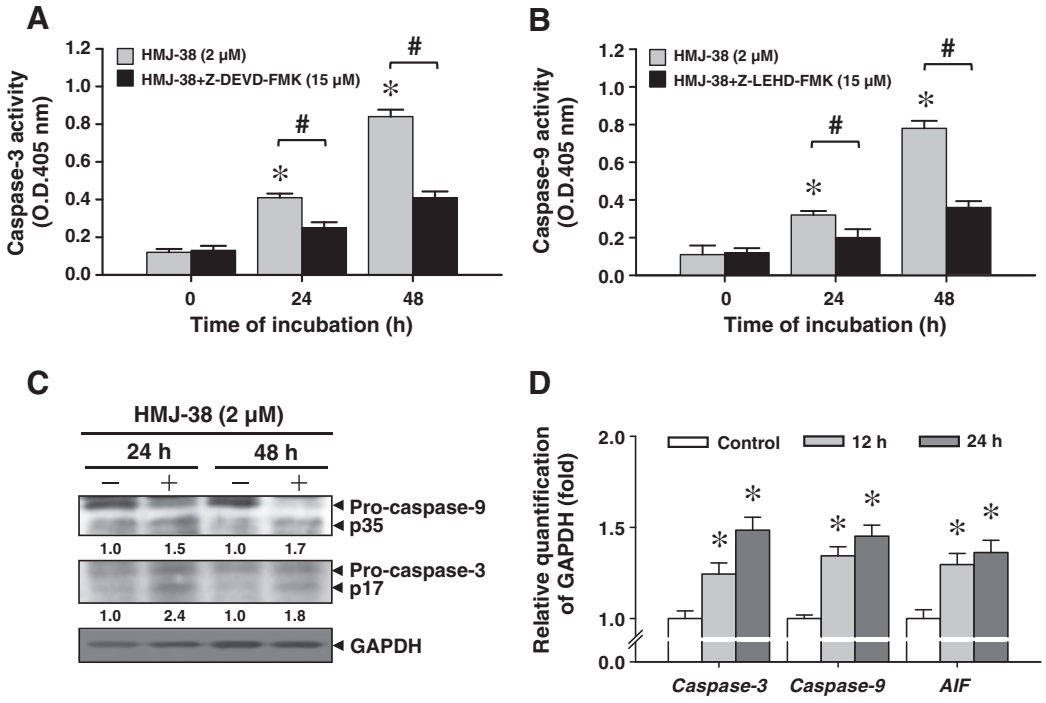

Fig. 3. HMJ-38 enhances the levels of caspase-3 and caspase-9 and activates intrinsic apoptotic signaling in CAL 27 cells. Cells were pretreated with or without 15 μM of Z-DEVD-FMK and Z-LEHD-FMK before exposure to 2 μM HMJ-38 for indicated periods of time. The whole-cell lysates were tested for (A) caspase-3 and (B) caspase-9 activities as described in Materials and methods. (C) Levels of caspase-9 and caspase-3 were examined by immunoblotting. (D) Total RNA was extracted, and quantitative RT-PCR analysis was performed using different specific primers. All results are calculated as mean ± S.E.M. (n = 3), and the difference is considered to be statistically significant by Dunnett's test. *$p < 0.05$ *versus* control cells; #$p < 0.05$ *versus* HMJ-38-treated samples.

3.3. CDK1-modulated Bcl-2 phosphorylation contributes to HMJ-38-enhanced CAL 27 cell apoptosis and mitotic arrest

To examine whether cell growth inhibition or viability in response to HMJ-38 challenge is associated with cell cycle arrest, DNA content was further assessed. Cell population in G_2/M phase markedly stagnated in HMJ-38-treated CAL 27 cells by 16.4, 39.6, 47.1 and 41.4% at 0, 12, 24 and 48 h, respectively (Fig. 4A and S1). G_2/M phase arrest reached a maximum at a 24-h challenge after HMJ-38 exposure. During incubation for the longer periods, HMJ-38 increased the manifestation of sub-G_1 population (apoptotic cells) in a time-dependent manner. We further explored if destruction of the microtubule organization is caused. Since our previous studies demonstrated that HMJ-38 can suppress tubulin polymerization and is considered an antimitotic agent [21,22]. The data in Fig. S2 indicated that treatments with HMJ-38 and colchicine for 24 h exhibited disruption and breakage of microtubule polymerization in the cytoplasm compared with that in control CAL 27 cells. In contrast, the maintenance of microtubule polymerization resulted from a 24-h paclitaxel exposure. Paclitaxel (a microtubule stabilization agent) and colchicine (a microtubule depolymerizing agent) were applied as reference compounds for the effect on mitotic spindle organization [43,44]. Additionally, HMJ-38 dramatically promoted CDK1 kinase activity for 3- to 24-h exposure (Fig. 4B). It is well known that the activity of CDK1/cyclin B1 kinase is tightly controlled when the cells enter mitotic phase [45,46]. Moreover, the microtubule-targeting agents (MTAs) provoked phosphorylation at the Thr161 site of CDK1, causing antiapoptotic response through Bcl-2 phosphorylated on Ser70 [43,44,47]. HMJ-38 increased the protein expressions of phospho-CDK1 (Thr161), CDK1 and phospho-Bcl-2 (Ser70) (Fig. 4C). We subsequently explored the role of CDK1 activation after HMJ-38 challenge. To find evidence whether CDK1 level alters the downstream signaling cascade, cells were preincubated with roscovitine and thereby exposed to HMJ-38. Roscovitine significantly abolished HMJ-38-reduced viability (Fig. 4D) and markedly decreased the number of TUNEL-positive cells (Fig. 4E). HMJ-38-triggered phospho-Bcl-2 (Ser70) protein expression was noticeably attenuated by roscovitine (Fig. 4F). Therefore, CDK1-mediated Bcl-2 phosphorylation might act as a functional link between mitotic arrest and apoptosis during *in vitro* cultivation of HMJ-38-incubated CAL 27 cells.

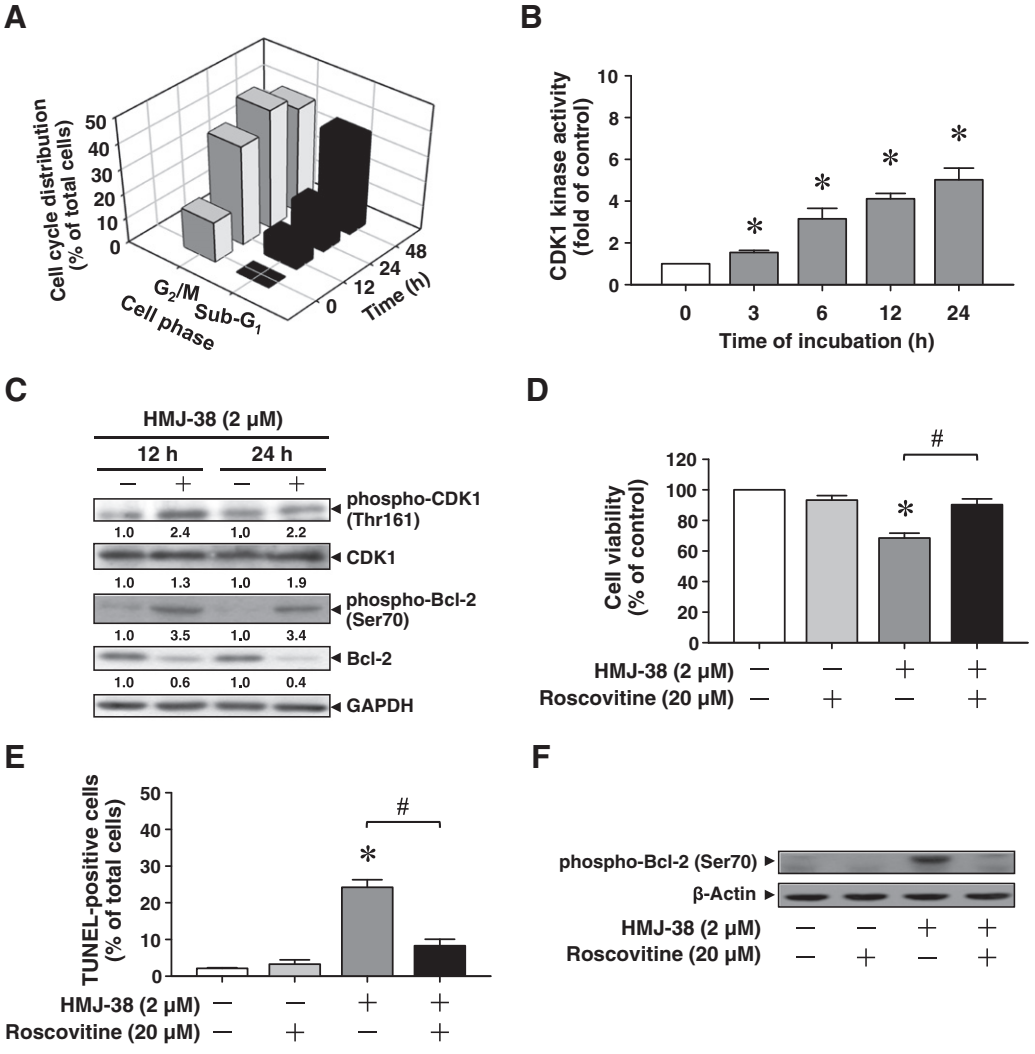

Fig. 4. HMJ-38 prompts apoptotic response *via* CDK1-regulated Bcl-2 phosphorylation in CAL 27 cells. Cells were treated with 2 μM HMJ-38 for different lengths of time. (A) Quantitative values for cell cycle distribution revealed DNA content (G_2/M phase and sub-G_1 population) performed as a three-dimensional (3-D) plot. (B) CDK1 kinase activity was measured as described in Materials and methods. (C) Cell lysates were subjected to Western blot for the detection of phospho-CDK1 (Thr161), CDK1, phospho-Bcl-2 (Ser70) and Bcl-2 protein levels. (D) Cell viability and (E) apoptotic death with TUNEL staining were individually determined for a 24-h exposure after 20 μM roscovitine preincubation. Results are given as mean ± S.E.M. (n = 3), and a significant difference is considered by Dunnett's test. *$p < 0.05$ *versus* control (0 h) value; #$p < 0.05$ *versus* HMJ-38-treated alone sample. (F) Cell fractions were employed for the level of phospho-Bcl-2 (Ser70) by immunoblotting.

3.4. HMJ-38 triggers proapoptotic ER stress response in CAL 27 cells

To explore the possibility that HMJ-38-induced apoptosis was employed through ER stress-mediated signaling, we set out to determine the level of intracellular Ca^{2+} in HMJ-38-treated cells for different intervals of time up to 24 h. HMJ-38 significantly promoted a time-dependent increase of cytoplasmic Ca^{2+} level at 6, 12 and 24-h treatments (Fig. 5A), indicating that HMJ-38 might stimulate UPR to trigger intracellular Ca^{2+} release and the apoptotic events. We further gained insight that HMJ-38-induced cytotoxic effect might be implicated in ER stress-mediated apoptosis. We subsequently explored both impacts on the biochemical upstream signals and Ca^{2+}-modulated relative mechanism. It has been reported that GADD153, an ER molecular chaperone, sensitizes ER stress process, and its upstream signal, like the phosphorylation of eIF2α on Ser51, plays a positive role [48,49]. Thereby, we also examined whether HMJ-38-induced UPR is correlated with calpain and caspase-4 as key regulators of ER stress during cell apoptosis [13,50]. HMJ-38 treatment resulted in up-regulation of associated protein levels, including GADD153, GRP78, ATF-6α, ATF-6β, eIF2α, phospho-eIF2α (Ser51), calpain 1 and caspase-4 (Fig. 5B). Cells after stimulation with HMJ-38 were observed to increase mRNA gene expression of *GADD153* and *GRP78* in a time-dependent response (Fig. 5C).

In addition, the accumulation of calpain activity was noticeably found in HMJ-38-treated cells when compared with untreated control cells (Fig. 5D). To confirm the role of ER stress-mediated apoptosis by HMJ-38, we pretreated CAL 27 cells with or without BAPTA (a Ca^{2+} chelator), calpeptin (a calpain specific inhibitor) or salubrinal (a selective inhibitor of eIF2α dephosphorylation) before exposure to HMJ-38 to investigate both of calpain 1 and viability. Calpeptin was effective on the inhibition of HMJ-38-enhanced calpain 1 (Fig. 5E). As expected,

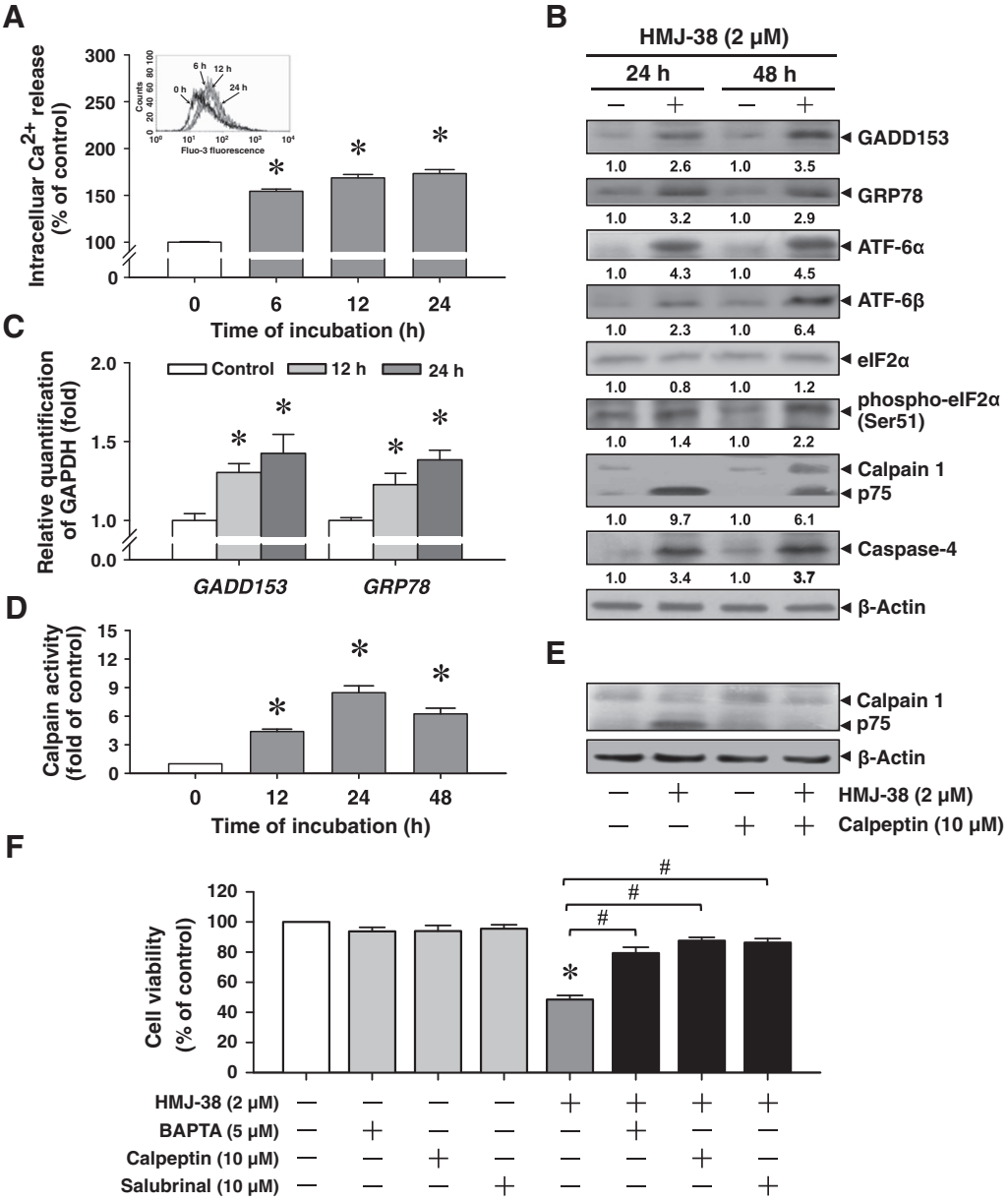

Fig. 5. Effects of intracellular Ca^{2+} release, calpain and phosphorylated eIF2α are required for HMJ-38-triggered ER stress and apoptosis on CAL 27 cells. Cells were pretreated with or without 10 μM of calpeptin or salubrinal, followed by stimulating with 2 μM HMJ-38 for various time periods. (A) Intracellular Ca^{2+} release was assessed by staining with Fluo-3/AM and flow cytometry. (B) Cells were collected and blotted using the specific antibodies for ER stress-modulated signal molecules [GADD153, GRP78, ATF-6α, ATF-6β, eIF2α, phospho-eIF2α (Ser51), calpain 1 and caspase-4]. (C) The gene levels of *GADD153* and *GRP78* were determined by quantitative RT-PCR method. (D) Cells were examined for calpain activity as described in Materials and methods. (E) The protein level of calpain l was examined by immunoblotting. (F) Cell viability was estimated by MTT assay. All values are expressed as mean ± S.E.M. (n = 3) and showed a significant difference by Dunnett's test. *$p < 0.05$ *versus* untreated control; #$p < 0.05$ *versus* HMJ-38 treatment only sample.

these compounds (BAPTA, calpeptin and salubrinal) significantly attenuated HMJ-38-reduced viability by up to 80% (Fig. 5F). Taken together, we provide bimolecular evidence regarding the influence of ER stress that contributed to HMJ-38-modulated cell death in CAL 27 cells.

3.5. HMJ-38 suppresses tumor growth of oral cancer xenografts

To further verify the possible anticancer mechanism of HMJ-38 *in vivo*, we performed a tumorigenicity assay in a murine xenograft model by subcutaneous transplantation with CAL 27 cells. Tumor-bearing mice were given HMJ-38 (1 and 2.5 mg/kg) by intraperitoneal injection for Q2D × 10 schedule or vehicle control. Representative picture of tumors with HMJ-38 administration to the mice revealed that significant therapeutic effect showed against xenograft tumor growth (Fig. 6A). HMJ-38 markedly decreased the tumor size (Fig. 6B) and weight (Fig. 6C) in treated animals in comparison to the control group. Moreover, there was a significant effect on the tumor inhibition rate, demonstrated by the ratio of 41.65% and 51.16% in both groups treated with HMJ-38 (1 and 2.5 mg/kg) as listed in Table S2. The xenograft tumors were also confirmed to probe the central apoptotic element as there was a rise in *caspase-3* gene expression (Fig. 6D) and an up-regulation of cleaved caspase-3 (Fig. 6E) in the 2.5 mg/kg HMJ-38 treatment group. Furthermore, no significant change was observed in mouse body weight after treatment with HMJ-38 (data not shown), indicating that there was no systemic toxicity. Importantly, no hepatotoxicity and renal toxicity were induced by HMJ-38 under the experimental conditions (Table S3). Collectively, we postulate that these xenografted suppressive responses *in vivo* exerted by HMJ-38 correlated with caspase-3-dependent mechanism identified *in vitro*.

4. Discussion

The present study found emerging evidence that HMJ-38 caused anticancer response against OSCC CAL 27 cells by the facilitation of mitotic arrest, ER stress and mitochondria-modulated apoptosis. The *in vivo* study also demonstrated that HMJ-38 attenuated tumor growth in CAL 27 xenografted nude mice. Hence, understanding the signal transduction of apoptotic death induced by HMJ-38 is vital to explore the

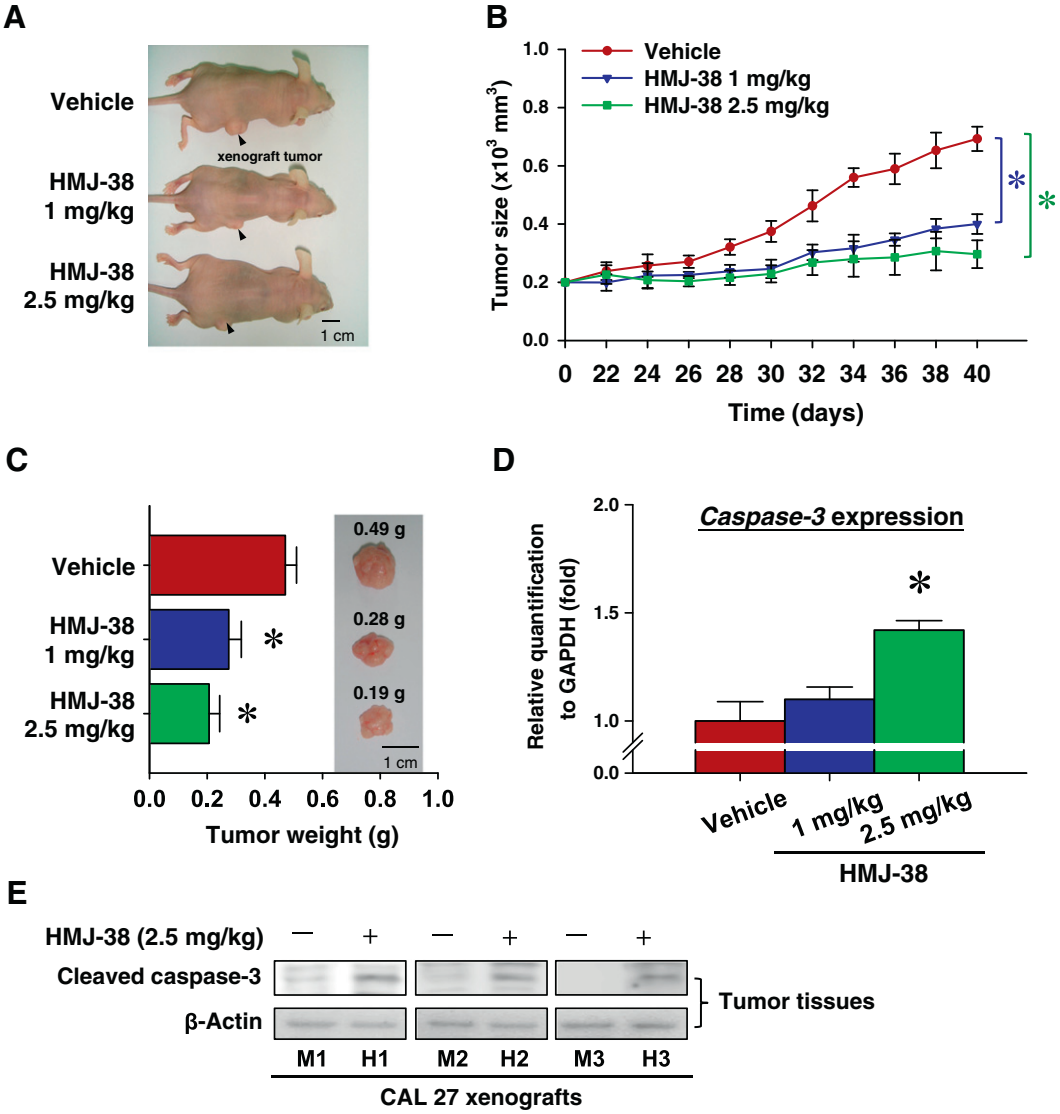

Fig. 6. HMJ-38 inhibits tumor growth and enhances caspase-3 expression in a CAL 27 cell ectopically xenograft model. After mice were subcutaneously injected with CAL 27 cells (1×10^7 cells/mouse) on the flank, the effects of HMJ-38 (1 and 2.5 mg/kg) were evaluated. (A) Representative animals with xenograft tumors were intraperitoneally administrated with or without HMJ-38. (B) Tumor size was measured every two days ten times and calculated for the duration of this experiment. (C) Tumor weight was taken upon euthanizing the mice and collecting the tumors. The values in bar graph represent mean ± S.E.M. from 8 animals of each group. Scale bar = 1 cm. (D) Quantitative RT-PCR analysis was used to probe the *caspase-3* gene from xenograft tumors. Results represent mean ± S.E.M. from at least five animals in each group. Asterisk (*) indicates the level of significant difference ($p < 0.05$ *versus* control group value) after testing by Dunnett's test. (E) Cell lysates from CAL 27 tumors were prepared, and the expression of cleaved caspase-3 protein was analyzed by Western blotting.

novel strategy for targeting chemotherapy. HMJ-38 deserves further investigation for preclinical study or clinical trial as a potential oral anticancer agent.

It has been reported that HMJ-38 possesses effective cytotoxic effect on multiple human tumor cell lines [22]. Our preliminary study investigated the cytotoxicity and *in vitro* antitumor effects on human oral cancer (CAL 27 and SCC-4) (Table 1) and leukemia cell lines (data not shown), respectively. In contrast, HMJ-38 exerts comparatively low efficacy against non-cancer cells, for example, PBMC [23] and human fibroblast cell lines (Table 1). HMJ-38 represents a promising candidate and exhibits anticancer property against neoplastic cells with low cytotoxic response in non-cancer cells. In addition, the current study provides novel information addressing the chemotherapy and an approach regarding HMJ-38 against human OSCC *in vitro* and *in vivo*. Our previous studies demonstrated that HMJ-38 is the most potent to continue interest in drug development [21–24]. Therefore, this study hypothesized that HMJ-38 might exhibit potential for treating drug-refractory cancers, such as HNSCC or OSCC.

The interference with microtubule assembly or disassembly exerts different dynamic aspects and represents crucial spectra for mode of action in antimitotic agents [51,52]. HMJ-38 and colchicine disrupted microtubule organization and displayed short microtubule fragments in the cytoplasm of CAL 27 cells (Fig. S2). Evidence indicates that CDK1 phosphorylates Bcl-2 at the Ser70 residue to suppress its antiapoptotic function [28,44]. In the present study, HMJ-38 dramatically promoted CDK1 kinase activity and up-regulated both phosphorylation of CDK1 and Bcl-2 proteins. Roscovitine prevented against HMJ-38-provoked apoptosis and abrogated phosphorylated Bcl-2 expression compared to treated cells (Fig. 4). Hence, HMJ-38-stimulated CDK1 activation might appear to be the action of phosphorylated Bcl-2 at the Ser70 site, resulting in the enhancement of mitotic arrest and apoptotic signaling. This finding is consistent with previous reports that the phosphorylation at the Thr161 site of CDK1 is likely to be stimulated by MTAs [43,47]. Consequently, HMJ-38-increased CDK1 activity might result from CDK-activating kinase modulation in CAL 27 cells *in vitro*. We previously demonstrated that the novel quinazolinone derivative, MJ-29, has a similar finding regarding the effect of CDK1-mediated Bcl-2 phosphorylation during cell apoptosis [28].

The current study further examined antitumor effect of HMJ-38 on CAL 27 cells by investigating apoptotic machinery. HMJ-38-triggered DNA fragmentation could be efficiently suppressed by Z-VAD-FMK (Fig. 1D and E), indicating that caspase cascade-dependent apoptosis occurred in HMJ-38-challenged cells. It is well documented that ER is a major place for protein folding, protein synthesis and cellular Ca^{2+} storage as a third subcellular compartment [14,15]. The misfolded proteins result in ER stress response to initiate imbalance in Ca^{2+} homeostasis, leading to activation of caspase cascade and ultimately cell apoptosis [17,53,54]. Particularly, the several reports have focused on ER stress-induced apoptosis for anticancer drug discovery [13,15]. GADD153 (CHOP) is a transcription factor and a crucial marker of ER stress; GRP78 also acts as an important ER chaperone in the occurrence of UPR [55–57]. HMJ-38 increased intracellular Ca^{2+} release and promoted calpain 1 protein level and calpain activity, showing that HMJ-38-provoked apoptotic effect was involved in Ca^{2+}-dependent regulation. Our finding also implied that an up-regulation of GADD153 and GRP78 at mRNA and protein levels appeared (Fig. 5B and C). Additionally, HMJ-38 prompted the levels of UPR-related protein expressions. Phosphorylated eIF2α-mediated ER stress has been known to implicate GADD153/CHOP signaling pathway [58,59]. Preincubation with salubrinal after HMJ-38 exposure diminished HMJ-38-reduced viability (Fig. 5F). Therefore, the event of ER stress response for apoptosis required the accumulation of unfolded or misfolded protein, and Ca^{2+} signaling provided a plausible explanation in HMJ-38-treated CAL 27 cells *in vitro*.

Mitochondrial dysfunction, one of the apoptotic targets, has been considered as an enter mechanism in apoptotic cell fate [15,18]. The previous study showed that reactive oxygen species (ROS) can cause mitochondrial depolarization and stimulate apoptotic caspase cascade signaling [56]. HMJ-38 facilitated loss of $\Delta\Psi m$ and MPT pore opening (Fig. 2A and B), and it thereafter stimulated the caspase-9 and caspase-3 activities (Fig. 3A and B), following initial activation of intrinsic apoptotic behavior. The mitochondrial function and the members of Bcl-2 family were also required for HMJ-38-induced apoptosis in CAL 27 cells. Furthermore, HMJ-38 enhanced ROS production in tested CAL 27 cells (data not shown). Thus, HMJ-38 triggered CAL 27 cell apoptosis through ROS generation and mitochondria-dependent effects. Specifically, this is the first study to prove that HMJ-38 effectively reduced tumor growth in CAL 27 xenografted mice with possibly exhibiting no adverse toxicity in the animals (Table S3). Strikingly, HMJ-38 also increased caspase-3 mRNA and protein levels in xenograft tumors *in vivo* (Fig. 6).

Our findings herein underscore that HMJ-38-sensitized CAL 27 cells mediating apoptotic death *in vitro* correlated to ER stress and intracellular Ca^{2+} release. We also report that mitochondrial dysfunction was triggered by HMJ-38 in an intrinsic pathway-mediated apoptotic mechanism of CAL 27 cells. In conclusion, these data support our hypothesis and clearly show that HMJ-38 inhibits the OSCC CAL 27 cells on the basis of the antitumor activity profiles of treatments both *in vitro* and *in vivo*. This study provides pharmacological evidence for apoptosis induced by HMJ-38 in oral cancer CAL 27 cells and the molecular root for cell-fate decision *in vitro* and *in vivo*.

Acknowledgements

The authors would like to thank Dr. Hsiu-Maan Kuo and Dr. Ya-Ling Lin (Department of Parasitology, China Medical University) for providing partial instruments. This work was supported by the Taiwan Department of Health, China Medical University Hospital Cancer Research Center of Excellence (DOH102-TD-C-111-005).

Appendix A. Supplementary data

Supplementary data to this article can be found online at http://dx.doi.org/10.1016/j.bbagen.2014.02.022.

References

[1] Y.J. Chen, S.C. Lin, T. Kao, C.S. Chang, P.S. Hong, T.M. Shieh, K.W. Chang, Genome-wide profiling of oral squamous cell carcinoma, J. Pathol. 204 (2004) 326–332.
[2] M. Pentenero, S. Gandolfo, M. Carrozzo, Importance of tumor thickness and depth of invasion in nodal involvement and prognosis of oral squamous cell carcinoma: a review of the literature, Head Neck 27 (2005) 1080–1091.
[3] S.Y. Liu, C.L. Lu, C.T. Chiou, C.Y. Yen, G.A. Liaw, Y.C. Chen, Y.C. Liu, W.F. Chiang, Surgical outcomes and prognostic factors of oral cancer associated with betel quid chewing and tobacco smoking in Taiwan, Oral Oncol. 46 (2010) 276–282.
[4] K. Sanjiv, T.L. Su, S. Suman, R. Kakadiya, T.C. Lai, H.Y. Wang, M. Hsiao, T.C. Lee, The novel DNA alkylating agent BO-1090 suppresses the growth of human oral cavity cancer in xenografted and orthotopic mouse models, Int. J. Cancer 130 (2012) 1440–1450.
[5] C. Muir, L. Weiland, Upper aerodigestive tract cancers, Cancer 75 (1995) 147–153.
[6] G.F. Funk, L.H. Karnell, R.A. Robinson, W.K. Zhen, D.K. Trask, H.T. Hoffman, Presentation, treatment, and outcome of oral cavity cancer: a National Cancer Data Base report, Head Neck 24 (2002) 165–180.
[7] F.S. Yu, J.S. Yang, C.S. Yu, C.C. Lu, J.H. Chiang, C.W. Lin, J.G. Chung, Safrole induces apoptosis in human oral cancer HSC-3 cells, J. Dent. Res. 90 (2011) 168–174.
[8] Y. Choi, S.Y. Kim, S.H. Kim, J. Yang, K. Park, Y. Byun, Inhibition of tumor growth by biodegradable microspheres containing all-trans-retinoic acid in a human head-and-neck cancer xenograft, Int. J. Cancer 107 (2003) 145–148.
[9] W.L. Lo, S.Y. Kao, L.Y. Chi, Y.K. Wong, R.C. Chang, Outcomes of oral squamous cell carcinoma in Taiwan after surgical therapy: factors affecting survival, J. Oral Maxillofac. Surg. 61 (2003) 751–758.
[10] Q. Sun, T. Sakaida, W. Yue, S.M. Gollin, J. Yu, Chemosensitization of head and neck cancer cells by PUMA, Mol. Cancer Ther. 6 (2007) 3180–3188.
[11] J.G. Chung, J.S. Yang, L.J. Huang, F.Y. Lee, C.M. Teng, S.C. Tsai, K.L. Lin, S.F. Wang, S.C. Kuo, Proteomic approach to studying the cytotoxicity of YC-1 on U937 leukemia cells and antileukemia activity in orthotopic model of leukemia mice, Proteomics 7 (2007) 3305–3317.
[12] G. Kroemer, L. Galluzzi, C. Brenner, Mitochondrial membrane permeabilization in cell death, Physiol. Rev. 87 (2007) 99–163.
[13] E. Lai, T. Teodoro, A. Volchuk, Endoplasmic reticulum stress: signaling the unfolded protein response, Physiology (Bethesda) 22 (2007) 193–201.

[14] I. Kim, W. Xu, J.C. Reed, Cell death and endoplasmic reticulum stress: disease relevance and therapeutic opportunities, Nat. Rev. Drug Discov. 7 (2008) 1013–1030.
[15] R. Kim, M. Emi, K. Tanabe, S. Murakami, Role of the unfolded protein response in cell death, Apoptosis 11 (2006) 5–13.
[16] Y.J. Chen, C.L. Wu, J.F. Liu, Y.C. Fong, S.F. Hsu, T.M. Li, Y.C. Su, S.H. Liu, C.H. Tang, Honokiol induces cell apoptosis in human chondrosarcoma cells through mitochondrial dysfunction and endoplasmic reticulum stress, Cancer Lett. 291 (2010) 20–30.
[17] C.M. Su, S.W. Wang, T.H. Lee, W.P. Tzeng, C.J. Hsiao, S.C. Liu, C.H. Tang, Trichodermin induces cell apoptosis through mitochondrial dysfunction and endoplasmic reticulum stress in human chondrosarcoma cells, Toxicol. Appl. Pharmacol. 272 (2013) 335–344.
[18] D.G. Breckenridge, M. Germain, J.P. Mathai, M. Nguyen, G.C. Shore, Regulation of apoptosis by endoplasmic reticulum pathways, Oncogene 22 (2003) 8608–8618.
[19] I.N. Lavrik, A. Golks, P.H. Krammer, Caspases: pharmacological manipulation of cell death, J. Clin. Invest. 115 (2005) 2665–2672.
[20] S. Orrenius, Reactive oxygen species in mitochondria-mediated cell death, Drug Metab. Rev. 39 (2007) 443–455.
[21] M.J. Hour, J.S. Yang, J.C. Lien, S.C. Kuo, L.J. Huang, Synthesis and cytotoxicity of 6-pyrrolidinyl-2-(2-substituted phenyl)-4-quinazolinones, J. Chin. Chem. Soc. 54 (2007) 785–790.
[22] M.J. Hour, L.J. Huang, S.C. Kuo, Y. Xia, K. Bastow, Y. Nakanishi, E. Hamel, K.H. Lee, 6-Alkylamino- and 2,3-dihydro-3′-methoxy-2-phenyl-4-quinazolinones and related compounds: their synthesis, cytotoxicity, and inhibition of tubulin polymerization, J. Med. Chem. 43 (2000) 4479–4487.
[23] J.S. Yang, M.J. Hour, S.C. Kuo, L.J. Huang, M.R. Lee, Selective induction of G2/M arrest and apoptosis in HL-60 by a potent anticancer agent, HMJ-38, Anticancer Res. 24 (2004) 1769–1778.
[24] J.H. Chiang, J.S. Yang, C.C. Lu, M.J. Hour, S.J. Chang, T.H. Lee, J.G. Chung, Newly synthesized quinazolinone HMJ-38 suppresses angiogenetic responses and triggers human umbilical vein endothelial cell apoptosis through p53-modulated Fas/death receptor signaling, Toxicol. Appl. Pharmacol. 269 (2013) 150–162.
[25] L. Jiang, N. Ji, Y. Zhou, J. Li, X. Liu, Z. Wang, Q. Chen, X. Zeng, CAL 27 is an oral adenosquamous carcinoma cell line, Oral Oncol. 45 (2009) e204–e207.
[26] M. Zhao, D. Sano, C.R. Pickering, S.A. Jasser, Y.C. Henderson, G.L. Clayman, E.M. Sturgis, T.J. Ow, R. Lotan, T.E. Carey, P.G. Sacks, J.R. Grandis, D. Sidransky, N.E. Heldin, J.N. Myers, Assembly and initial characterization of a panel of 85 genomically validated cell lines from diverse head and neck tumor sites, Clin. Cancer Res. 17 (2011) 7248–7264.
[27] C.C. Lu, J.S. Yang, J.H. Chiang, M.J. Hour, S. Amagaya, K.W. Lu, J.P. Lin, N.Y. Tang, T.H. Lee, J.G. Chung, Inhibition of invasion and migration by newly synthesized quinazolinone MJ-29 in human oral cancer CAL 27 cells through suppression of MMP-2/9 expression and combined down-regulation of MAPK and AKT signaling, Anticancer Res. 32 (2012) 2895–2903.
[28] J.S. Yang, M.J. Hour, W.W. Huang, K.L. Lin, S.C. Kuo, J.G. Chung, MJ-29 inhibits tubulin polymerization, induces mitotic arrest, and triggers apoptosis *via* cyclin-dependent kinase 1-mediated Bcl-2 phosphorylation in human leukemia U937 cells, J. Pharmacol. Exp. Ther. 334 (2010) 477–488.
[29] C.C. Lu, J.S. Yang, J.H. Chiang, M.J. Hour, K.L. Lin, J.J. Lin, W.W. Huang, M. Tsuzuki, T.H. Lee, J.G. Chung, Novel quinazolinone MJ-29 triggers endoplasmic reticulum stress and intrinsic apoptosis in murine leukemia WEHI-3 cells and inhibits leukemic mice, PLoS One 7 (2012) e36831.
[30] J.H. Chiang, J.S. Yang, C.Y. Ma, M.D. Yang, H.Y. Huang, T.C. Hsia, H.M. Kuo, P.P. Wu, T.H. Lee, J.G. Chung, Danthron, an anthraquinone derivative, induces DNA damage and caspase cascades-mediated apoptosis in SNU-1 human gastric cancer cells through mitochondrial permeability transition pores and Bax-triggered pathways, Chem. Res. Toxicol. 24 (2011) 20–29.
[31] H. Lee, M.T. Park, B.H. Choi, E.T. Oh, M.J. Song, J. Lee, C. Kim, B.U. Lim, H.J. Park, Endoplasmic reticulum stress-induced JNK activation is a critical event leading to mitochondria-mediated cell death caused by beta-lapachone treatment, PLoS One 6 (2011) e21533.
[32] C.C. Lu, J.S. Yang, A.C. Huang, T.C. Hsia, S.T. Chou, C.L. Kuo, H.F. Lu, T.H. Lee, W.G. Wood, J.G. Chung, Chrysophanol induces necrosis through the production of ROS and alteration of ATP levels in J5 human liver cancer cells, Mol. Nutr. Food Res. 54 (2010) 967–976.
[33] B.C. Ji, W.H. Hsu, J.S. Yang, T.C. Hsia, C.C. Lu, J.H. Chiang, J.L. Yang, C.H. Lin, J.J. Lin, L.J. Suen, W. Gibson Wood, J.G. Chung, Gallic acid induces apoptosis *via* caspase-3 and mitochondrion-dependent pathways *in vitro* and suppresses lung xenograft tumor growth *in vivo*, J. Agric. Food Chem. 57 (2009) 7596–7604.
[34] C.C. Lin, Y.J. Chuang, C.C. Yu, J.S. Yang, C.C. Lu, J.H. Chiang, J.P. Lin, N.Y. Tang, A.C. Huang, J.G. Chung, Apigenin induces apoptosis through mitochondrial dysfunction in U-2 OS human osteosarcoma cells and inhibits osteosarcoma xenograft tumor growth *in vivo*, J. Agric. Food Chem. 60 (2012) 11395–11402.
[35] Y. Dong, J. Tan, M.Z. Cui, G. Zhao, G. Mao, N. Singh, X. Xu, Calpain inhibitor MDL28170 modulates Abeta formation by inhibiting the formation of intermediate Abeta46 and protecting Abeta from degradation, FASEB J. 20 (2006) 331–333.
[36] J.F. Liu, Y.C. Fong, K.W. Chang, S.C. Kuo, C.S. Chang, C.H. Tang, FPTB, a novel CA-4 derivative, induces cell apoptosis of human chondrosarcoma cells through mitochondrial dysfunction and endoplasmic reticulum stress pathways, J. Cell. Biochem. 112 (2011) 453–462.
[37] S. Nam, D.M. Smith, Q.P. Dou, Tannic acid potently inhibits tumor cell proteasome activity, increases p27 and Bax expression, and induces G1 arrest and apoptosis, Cancer Epidemiol. Biomarkers Prev. 10 (2001) 1083–1088.
[38] C. Muraki, N. Ohga, Y. Hida, H. Nishihara, Y. Kato, K. Tsuchiya, K. Matsuda, Y. Totsuka, M. Shindoh, K. Hida, Cyclooxygenase-2 inhibition causes antiangiogenic effects on tumor endothelial and vascular progenitor cells, Int. J. Cancer 130 (2012) 59–70.
[39] P. Boya, I. Cohen, N. Zamzami, H.L. Vieira, G. Kroemer, Endoplasmic reticulum stress-induced cell death requires mitochondrial membrane permeabilization, Cell Death Differ. 9 (2002) 465–467.
[40] J. Moungjaroen, U. Nimmannit, P.S. Callery, L. Wang, N. Azad, V. Lipipun, P. Chanvorachote, Y. Rojanasakul, Reactive oxygen species mediate caspase activation and apoptosis induced by lipoic acid in human lung epithelial cancer cells through Bcl-2 down-regulation, J. Pharmacol. Exp. Ther. 319 (2006) 1062–1069.
[41] E. Pozo-Guisado, J.M. Merino, S. Mulero-Navarro, M.J. Lorenzo-Benayas, F. Centeno, A. Alvarez-Barrientos, P.M. Fernandez-Salguero, Resveratrol-induced apoptosis in MCF-7 human breast cancer cells involves a caspase-independent mechanism with downregulation of Bcl-2 and NF-kappaB, Int. J. Cancer 115 (2005) 74–84.
[42] G.Y. Zhu, Y.W. Li, A.K. Tse, D.K. Hau, C.H. Leung, Z.L. Yu, W.F. Fong, 20(S)-Protopanaxadiol, a metabolite of ginsenosides, induced cell apoptosis through endoplasmic reticulum stress in human hepatocarcinoma HepG2 cells, Eur. J. Pharmacol. 668 (2011) 88–98.
[43] Y.T. Huang, D.M. Huang, J.H. Guh, I.L. Chen, C.C. Tzeng, C.M. Teng, CIL-102 interacts with microtubule polymerization and causes mitotic arrest following apoptosis in the human prostate cancer PC-3 cell line, J. Biol. Chem. 280 (2005) 2771–2779.
[44] L.G. Wang, X.M. Liu, W. Kreis, D.R. Budman, The effect of antimicrotubule agents on signal transduction pathways of apoptosis: a review, Cancer Chemother. Pharmacol. 44 (1999) 355–361.
[45] S.F. Kan, W.J. Huang, L.C. Lin, P.S. Wang, Inhibitory effects of evodiamine on the growth of human prostate cancer cell line LNCaP, Int. J. Cancer 110 (2004) 641–651.
[46] A.W. Murray, Recycling the cell cycle: cyclins revisited, Cell 116 (2004) 221–234.
[47] D. Yu, T. Jing, B. Liu, J. Yao, M. Tan, T.J. McDonnell, M.C. Hung, Overexpression of ErbB2 blocks Taxol-induced apoptosis by upregulation of p21Cip1, which inhibits p34Cdc2 kinase, Mol. Cell 2 (1998) 581–591.
[48] K.D. McCullough, J.L. Martindale, L.O. Klotz, T.Y. Aw, N.J. Holbrook, Gadd153 sensitizes cells to endoplasmic reticulum stress by down-regulating Bcl2 and perturbing the cellular redox state, Mol. Cell. Biol. 21 (2001) 1249–1259.
[49] S. Oyadomari, M. Mori, Roles of CHOP/GADD153 in endoplasmic reticulum stress, Cell Death Differ. 11 (2004) 381–389.
[50] S. Matsuzaki, T. Hiratsuka, R. Kuwahara, T. Katayama, M. Tohyama, Caspase-4 is partially cleaved by calpain *via* the impairment of Ca2+ homeostasis under the ER stress, Neurochem. Int. 56 (2010) 352–356.
[51] E.A. Perez, Microtubule inhibitors: differentiating tubulin-inhibiting agents based on mechanisms of action, clinical activity, and resistance, Mol. Cancer Ther. 8 (2009) 2086–2095.
[52] K.L. Cheng, T. Bradley, D.R. Budman, Novel microtubule-targeting agents — the epothilones, Biogeosciences 2 (2008) 789–811.
[53] A. Deniaud, O. Sharaf el dein, E. Maillier, D. Poncet, G. Kroemer, C. Lemaire, C. Brenner, Endoplasmic reticulum stress induces calcium-dependent permeability transition, mitochondrial outer membrane permeabilization and apoptosis, Oncogene 27 (2008) 285–299.
[54] H.K. Baumgartner, J.V. Gerasimenko, C. Thorne, P. Ferdek, T. Pozzan, A.V. Tepikin, O.H. Petersen, R. Sutton, A.J. Watson, O.V. Gerasimenko, Calcium elevation in mitochondria is the main $Ca2^{+}$ requirement for mitochondrial permeability transition pore (mPTP) opening, J. Biol. Chem. 284 (2009) 20796–20803.
[55] K.F. Ferri, G. Kroemer, Organelle-specific initiation of cell death pathways, Nat. Cell Biol. 3 (2001) E255–E263.
[56] Y.F. Kuo, Y.Z. Su, Y.H. Tseng, S.Y. Wang, H.M. Wang, P.J. Chueh, Flavokawain B, a novel chalcone from *Alpinia pricei* Hayata with potent apoptotic activity: involvement of ROS and GADD153 upstream of mitochondria-dependent apoptosis in HCT116 cells, Free Radic. Biol. Med. 49 (2010) 214–226.
[57] H.Y. Lin, P. Masso-Welch, Y.P. Di, J.W. Cai, J.W. Shen, J.R. Subjeck, The 170-kDa glucose-regulated stress protein is an endoplasmic reticulum protein that binds immunoglobulin, Mol. Biol. Cell 4 (1993) 1109–1119.
[58] O. Donze, R. Jagus, A.E. Koromilas, J.W. Hershey, N. Sonenberg, Abrogation of translation initiation factor eIF-2 phosphorylation causes malignant transformation of NIH 3T3 cells, EMBO J. 14 (1995) 3828–3834.
[59] M. Boyce, K.F. Bryant, C. Jousse, K. Long, H.P. Harding, D. Scheuner, R.J. Kaufman, D. Ma, D.M. Coen, D. Ron, J. Yuan, A selective inhibitor of eIF2alpha dephosphorylation protects cells from ER stress, Science 307 (2005) 935–939.